



Impact of 3-D Earth structure on Fennoscandian glacial isostatic adjustment: Implications for space-geodetic estimates of present-day crustal deformations

Pippa Whitehouse,¹ Konstantin Letychev,² Glenn A. Milne,¹ Jerry X. Mitrovica,² and Roblyn Kendall²

Received 11 April 2006; revised 22 May 2006; accepted 25 May 2006; published 7 July 2006.

[1] The importance of including lateral Earth structure in the analysis of Fennoscandian glacial isostatic adjustment (GIA) is investigated using a finite volume numerical formulation. Comparing output from radially-varying 1-D Earth models and models which account for the presence of plate boundaries, lateral variations in lithospheric thickness and viscosity heterogeneities in the upper and lower mantle, we find that perturbations to present-day rates of surface deformation due to the inclusion of 3-D Earth structure significantly exceed current observational uncertainties. Predicted residuals between 1-D and 3-D Earth models may be improved with the use of a 1-D model which approximates the local depth-dependent mean of the 3-D model. However, the remaining misfit is still large enough to significantly bias inferences of Earth structure and ice history. We conclude that lateral variations at both global and regional scales must be accounted for when interpreting GPS observations from Fennoscandia. **Citation:** Whitehouse, P., K. Letychev, G. A. Milne, J. X. Mitrovica, and R. Kendall (2006), Impact of 3-D Earth structure on Fennoscandian glacial isostatic adjustment: Implications for space-geodetic estimates of present-day crustal deformations, *Geophys. Res. Lett.*, 33, L13502, doi:10.1029/2006GL026568.

1. Introduction

[2] The recent geodynamic history of Fennoscandia is dominated by GIA and is manifest in a broad set of observables. These observations have traditionally included records of sea level change since the Last Glacial Maximum [Lambeck *et al.*, 1998] and over the last century [Ekman, 1996], and present-day anomalies in the Earth's gravitational field. More recently, these data sets have been extended to include estimates of ongoing 3-D crustal motion obtained through surveying by the Global Positioning System (GPS) [Johansson *et al.*, 2002].

[3] Previous analyses of Earth structure from these observations have focussed, almost exclusively, on 1-D models defined by the thickness of an elastic lithosphere and a radial profile of mantle viscosity [e.g., Fjeldskaar and Cathles, 1991; Mitrovica, 1996; Lambeck *et al.*, 1998; Davis *et al.*, 1999; Kaufmann and Lambeck, 2002; Milne *et al.*, 2001]. However, there is clear evidence for the

existence of significant lateral variation in Earth structure beneath Fennoscandia. As an example, Bungum *et al.* [1980] used teleseismic P-wave arrivals to identify Moho depths in the range 28–45 km across this region, while early studies of Rayleigh wave dispersion data indicated that the thickness of the lithosphere varies from 110 km beneath the coast of Norway to 170 km in central Finland [Calcagnile, 1982]. Coherence studies also indicate a strong east-west gradient in flexural rigidity corresponding to a variation in elastic thickness of approximately 80 km [Poudjom Djomani *et al.*, 1999]. Moreover, global [e.g., Ritsema *et al.*, 2004] and regional [Sandoval *et al.*, 2004] high resolution body-wave tomography has also revealed significant lateral structure in the upper and lower mantle beneath the Baltic shield.

[4] A small number of studies have moved beyond 1-D Earth models to analyze Fennoscandian GIA. Martinec and Wolf [2005] used a model with an axisymmetric lithospheric root and ice load to analyze the so-called Fennoscandian relaxation spectrum. They argued that the data set was consistent with a 200 km lithosphere below central Fennoscandia and 80 km at the periphery. Kaufmann *et al.* [2000] used a flat Earth model with realistic variations in lithospheric thickness and asthenospheric viscosity, and concluded that such structure has significant impact on predictions of relative sea level changes, uplift rates and gravity anomalies. In an extension to this work, Kaufmann and Wu [2002] used synthetic data generated using the 3-D model to assess the potential impact of such structure on inferences of a best-fitting 1-D Earth model.

[5] The growing recognition of the importance of 3-D structure on the GIA process [e.g., Steffen and Kaufmann, 2005] has motivated the development of numerical methods of increasing complexity. Indeed, numerical methods that allow for the incorporation of both realistic 3-D variations in viscoelastic Earth structure and an arbitrary ice load history have been described in the literature [e.g., Martinec, 2000; Zhong *et al.*, 2003; Letychev *et al.*, 2005a] and these models have been interfaced with methods for treating a complementary, gravitationally self-consistent ocean redistribution [Wu and van der Wal, 2003; Wu *et al.*, 2005; Paulson *et al.*, 2005].

[6] In this paper we consider the impact of 3-D variations in Earth structure on predictions of present-day crustal velocities in Fennoscandia using the finite-volume formalism described by Letychev *et al.* [2005a]. The study is motivated by the increasingly accurate constraints on the deformation field that are being obtained by the BIFROST continuous GPS network [Johansson *et al.*, 2002]. The

¹Department of Earth Sciences, University of Durham, Durham, UK.

²Department of Physics, University of Toronto, Toronto, Ontario, Canada.

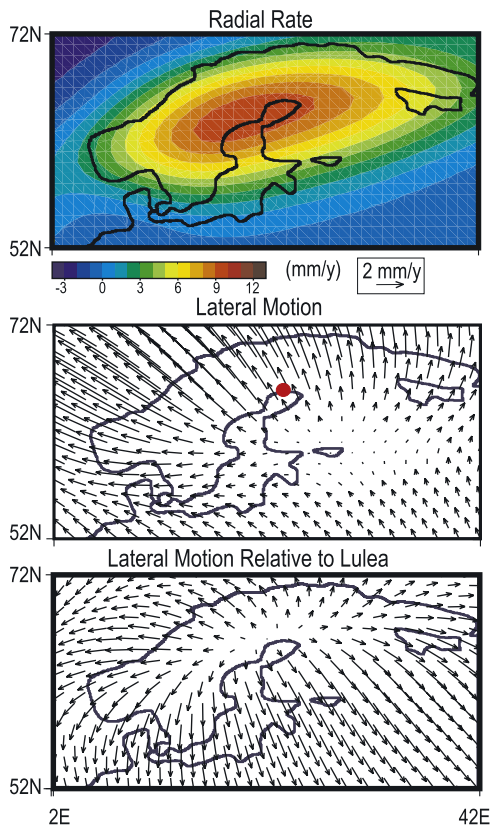


Figure 1. (top) GIA-induced present-day radial and (middle) tangential crustal velocities predicted using the radial reference model RR defined in the text. (bottom) The tangential velocities relative to the site Lulea, Sweden, the location of which is given by the red dot in Figure 1 (middle).

BIFROST network was deployed between 1993 and 1997 and *Johansson et al.* [2002] cited errors in the horizontal and vertical rates as small as 0.1 mm/yr and 0.5 mm/yr respectively. *Milne et al.* [2001] analyzed these rates using 1-D Earth models and, while their best-fitting model was able to capture the basic elements of the regional deformation field (see below), they noted several systematic discrepancies. The goals of our analysis are: to assess whether perturbations associated with 3-D Earth structure exceed the current observational uncertainties; to isolate sensitivities associated with plate boundaries, lithospheric thickness variations, and viscosity heterogeneity within both the upper and lower mantle; and to consider whether these perturbations might be mimicked by a change in the underlying radial Earth model, and thus whether such structure can bias 1-D inferences. More generally, our goal is to provide guidance to ongoing efforts to constrain GIA models using space-geodetic surveying.

2. Results

[7] All of the results presented here are based on the 3-D self-gravitating, viscoelastic Earth model outlined by *Latychev et al.* [2005a]. This formulation incorporates elastic compressibility, which is known to be important for obtaining accurate predictions of horizontal motions

[*Mitrović et al.*, 1994]. The elastic structure is prescribed by the seismically constrained PREM [*Dziewonski and Anderson*, 1981]. The surface mass load is comprised of a realistic ice model and a complementary water load. The former is constructed by combining the Fennoscandian ice history inferred by *Lambeck et al.* [1998] with the non-Fennoscandian components of the global ICE-3G deglaciation history [*Tushingham and Peltier*, 1991]. The Fennoscandian ice history of *Lambeck et al.* [1998] was tuned to provide a good fit to a large suite of local sea-level curves, and it has been shown to yield a best-fit to BIFROST GPS rates [*Milne et al.*, 2004].

2.1. Spherically Symmetric Results

[8] We begin by showing predictions based on a spherically symmetric (i.e., 1-D) Earth model which is, within this class of models, known to provide close to a best-fit to the BIFROST-determined 3-D crustal velocities (Figure 1). The model, our so-called radial reference Earth model (RR) is defined by an elastic lithosphere of thickness 120 km, an upper mantle viscosity of 5×10^{20} Pa s, and a lower mantle viscosity of 5×10^{21} Pa s. The radial velocity field is characterized by a zone of post-glacial uplift, with peak rates of 10 mm/yr in the northern Gulf of Bothnia, near the BIFROST site Lulea, Sweden (red dot in Figure 1 (middle)). This zone is surrounded by peripheral subsidence of several mm/yr in the Norwegian Sea and northern Europe.

[9] For this particular Earth model, the horizontal motions have a general southeast to northwest trend, with rates exceeding 2 mm/yr in Norway (Figure 1 (middle)). The trend is a consequence of deformation toward Canada driven by deglaciation of the Laurentian ice sheet. This ‘far-field’ effect can be removed by plotting the horizontal motions relative to the prediction at Lulea (Figure 1 (bottom)), to leave a characteristic divergent (from the center of rebound) pattern that has been described elsewhere [*James and Lambert*, 1993; *Mitrović et al.*, 1994]. *Mitrović et al.* [1994] showed that horizontal motions over Fennoscandia driven by Laurentian deglaciation become significantly more pronounced as the lower mantle viscosity is increased from $\sim 10^{21}$ Pa s to 5×10^{21} Pa s, and this explains the ‘far-field contamination’ evident in moving from the Figure 1 (bottom) to Figure 1 (middle) (see *James* [1991] for a discussion of the physics of GIA-induced horizontal motions). Conversely, the contamination is sufficiently small for models with lower mantle viscosity of $\sim 10^{21}$ Pa s, that the total prediction (not simply relative to Lulea) has the general pattern evident in Figure 1 (bottom). In subsequent discussions we will show both total and relative-to-Lulea horizontal motions in order to discriminate between local and far-field effects. (Of course, this separation is not perfect, since all such plots will by definition show zero horizontal motion at Lulea, and the Lulea prediction may not represent the ‘mean’ far-field effect over Fennoscandia associated with Laurentian unloading.)

2.2. 3-D Earth Models

[10] Our 3-D Earth models incorporate global perturbations to both the lithospheric thickness and the mantle viscosity. The former, plotted over Europe and the northeast Atlantic, is shown in Figure 2 (left). The lithospheric thickness variation is derived from estimates of elastic

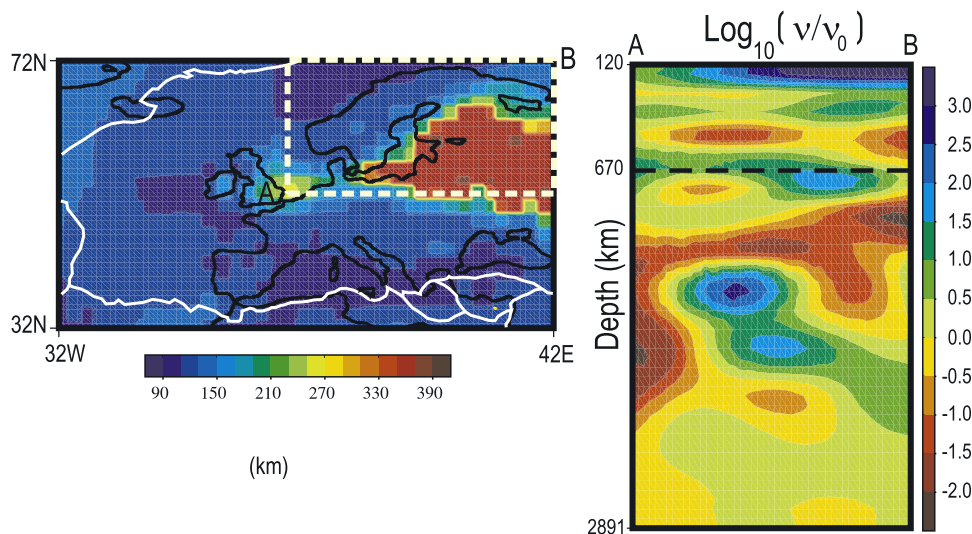


Figure 2. (left) Lithospheric thickness variations (color contours) from *Watts* [2001] and plate boundaries (white lines) incorporated into the 3-D GIA simulations described in the text. Only the portion of the global structure over the North Atlantic and Europe is shown. Figures 1, 3, and 4 show results within the geographic zone defined by the box at top right. (right) Viscosity variations relative to the radial reference model (RR) adopted in the 3-D GIA calculations. Assuming a constant lithospheric thickness of 120 km, the variations are shown for a vertical cross-section extending from 120 km depth to the base of the mantle (the dashed line shows the discontinuity at 670 km depth that defines the boundary between the upper and lower mantle) and oriented along a profile extending from points A to B in Figure 2 (left).

thickness presented in the global study of *Watts* [2001] and the regional analysis of *Pérez-Gussinyé et al.* [2004]. The principle inference for Fennoscandian structure is a steep increase in thickness across the Gulf of Bothnia and southern Finland. The 3-D model which includes lateral structure in the lithosphere only will be denoted model LT (the global mean lithospheric thickness of model LT is tuned to the value of the radial reference model RR, 120 km). A second aspect of lithospheric structure is explored by model PB, which is defined by plate boundary weak zones (Figure 2 (left), white lines) superimposed on the reference model RR. Following *Latychev et al.* [2005b], these zones are constructed by introducing a 200 km wide region of low (2×10^{20} Pa s) viscosity into the lithosphere structure.

[11] The 3-D mantle viscosity field is ultimately derived from a global seismic shear wave velocity model [*Ritsema et al.*, 2004] using the approach discussed in detail by *Latychev et al.* [2005a]. The viscosity field is generated from this model in a sequence of steps: first, a velocity-to-density scaling is applied; second, the density perturbation is converted to a temperature variation using a coefficient of thermal expansion; third, a simple exponential dependence is assumed to map temperature variations into viscosity variations. Finally, a radially dependent scaling is applied to this viscosity field to ensure that the global, depth-dependent logarithmic mean of the 3-D viscosity field is identical to model RR. Figure 2 (right) shows a vertical cross-section through the viscosity field along a great circle profile from geographic points A-B (see Figure 2 (left)). This plot shows a high viscosity root structure underlying the Fennoscandian lithosphere and, at greater depths, lateral variations which reach ~ 3 and ~ 5 orders of magnitude in the upper and lower mantle, respectively. We define two different 3-D models on the basis of this field; UM and LM denote models which incorporate viscosity variations only within the upper and lower mantle, respectively.

[12] Figure 3 (top) shows results generated by combining all aspects of the 3-D Earth models LT, PB, UM and LM (i.e., lithospheric thickness and whole mantle viscosity variations, as well as plate boundaries; hereinafter referred to as model FL). The predictions are shown relative to the results for the reference model RR, and thus represent perturbations associated with 3-D structure. The peak radial and tangential rate perturbations exceed 3 mm/yr and 1 mm/yr respectively over Fennoscandia, these are nearly an order of magnitude greater than the BIFROST uncertainty as of 2002 [*Johansson et al.*, 2002]. We conclude that 3-D structure must be included in the GIA analysis of the space-geodetic data set.

[13] We have performed a suite of predictions based on spherically symmetric Earth models with two-layer (upper mantle, lower mantle) viscosity profiles to determine whether the perturbation FL-RR may be mimicked by a revision to the 1-D Earth model RR. We found that the best two-layer model yielded fits to the 3-D predictions FL that were comparable to two other multi-layer (but 1-D) viscosity profiles considered. The first was the 1-D model generated by taking the arithmetic mean of lithospheric structure and the logarithmic mean of mantle structure within the geographic region defined by the rectangular domain shown in Figure 2. We denote this model RR2. The second was a model derived from a least-squares inversion of the FL predictions for a 1-D (multi-layer) viscosity profile. As an example of these results, the perturbation FL-RR2 is shown on Figure 3 (bottom), where we note that the amplitude of the discrepancy is reduced by a factor of two relative to Figure 3 (top). The discrepancies still exceed the uncertainties cited by *Johansson et al.* [2002] by a factor of 5 and thus we conclude that no 1-D Earth model is able to mimic the 3-D predictions FL to within the error associated with the BIFROST determined rates.

[14] These results have important implications for efforts to constrain models of Fennoscandian deglaciation history

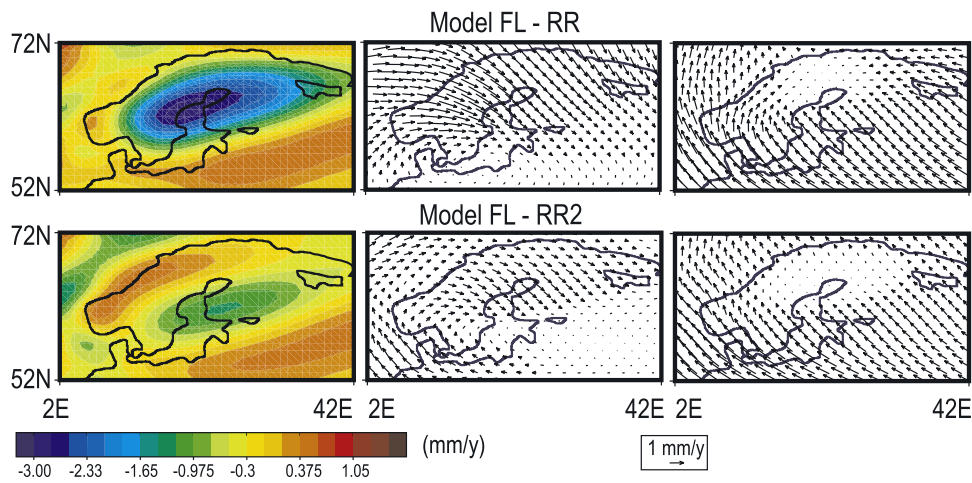


Figure 3. (top) The predicted difference between (left) GIA-induced present-day radial and (middle) tangential crustal velocities generated using the 3-D Earth model FL and the radial reference model RR. (right) The results of Figure 3 (middle) relative to the perturbation at Lulea, Sweden (the location of this site is given in Figure 1 (middle)). (bottom) As for Figure 3 (top) except the perturbation is shown relative to the 1-D radial Earth model RR2.

using GPS data. Consider, for example, discrepancies in the vertical rates associated with lateral structure. As indicated in Figure 3 (left), regardless of the 1-D viscosity model employed, there will remain a significant residual signal. Therefore, the only way to fit the GPS data with a 1-D model would be by varying the ice history. The specific bias

incurred will depend on the lithospheric thickness and viscosity structure adopted in the 1-D model. For example, application of the model RR2 would result in an ice model with ice thicknesses that are underestimated in the Gulf of Bothnia and northern Finland and overestimated within most of Norway and southeast of Finland.

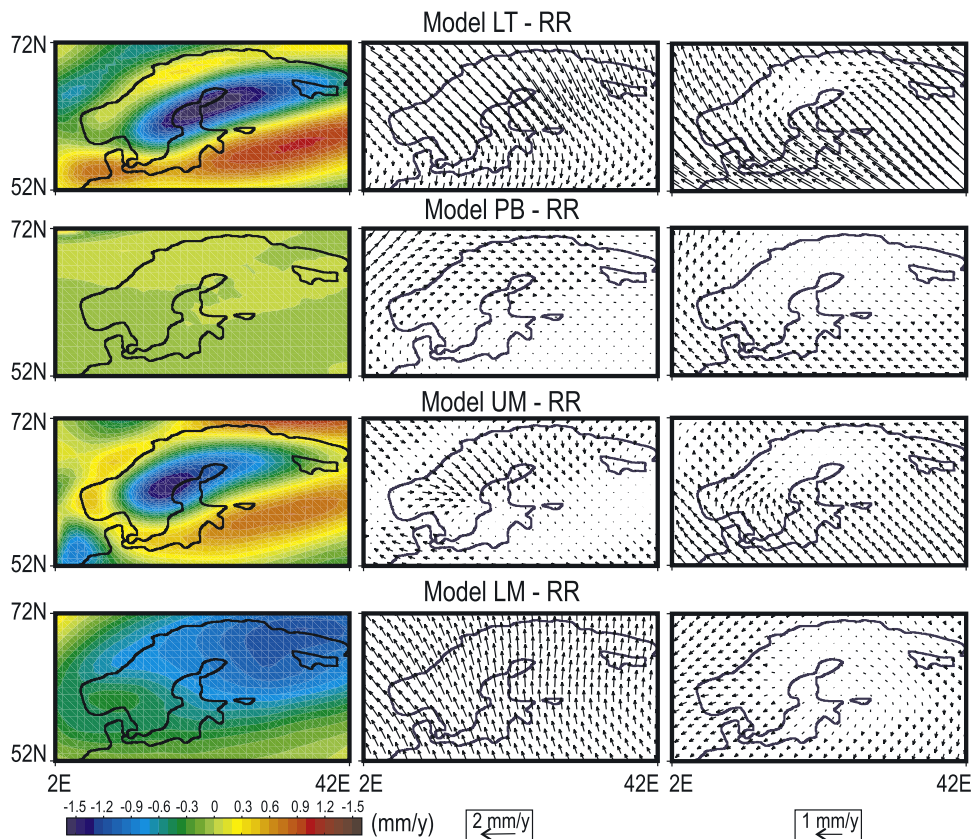


Figure 4. The predicted difference between (left) GIA-induced present-day radial and (middle) tangential crustal velocities generated using a laterally varying Earth model (LT, PB, UM, or LM, as defined in the text) and the radial reference model RR. (right) The results of Figure 4 (middle) relative to the result for Lulea, Sweden (see Figure 1).

[15] Next we have performed 3-D predictions based on the individual models LT, PB, UM and LM in order to explore the origin of the ‘total’ discrepancies evident in Figure 3. These results are shown in Figure 4 relative to the reference model RR.

[16] With regard to the radial component of the predictions (Figure 4 (left)), contributions from models LT and UM are highly correlated and dominate the discrepancies associated with the model FL (Figure 3 (top left)). The signal associated with lower mantle heterogeneity displays a different pattern, with longer wavelength structure and smaller amplitude. Plate boundary effects are close to zero and lie within the observational uncertainty.

[17] The influence of plate boundaries on horizontal motions is more significant (middle column), with a southwest to northeast gradient across Fennoscandia evident in the differential rates (right column). The relative-to-Lulea signals associated with lithospheric thickness variations and upper mantle viscosity heterogeneity are correlated and they dominate the ‘total’ signal derived using model FL (Figure 3 (top right)). The influence of structure in the lower mantle is, once again, distinct from the other effects, with a northward trending perturbation that rotates to northwest in the southwestern sector of Fennoscandia. In any event, each of the four components of 3-D Earth structure yield signals that exceed the observational uncertainty for horizontal motion.

[18] The results in Figures 3 and 4 indicate that both far-field and near-field lateral structure contribute significantly to the predicted Fennoscandian velocity field. The far-field structure appears to be more significant when predicting horizontal motions. The distinct sensitivity of the predictions to lower mantle structure suggests that it might be possible to infer such structure given suitably accurate observations; although inferences of this kind will have to account for uncertainties in the regional ice history. In contrast, the signals associated with lateral variations in the lithosphere and upper mantle are well correlated, and thus the structure in these two layers will likely not be separable using GPS data alone.

[19] **Acknowledgments.** We thank Tony Watts for making his global elastic thickness model available to us and Kurt Lambeck for making his Fennoscandian ice model available to us. We also thank an anonymous reviewer for constructive and helpful comments.

References

Bungum, H., S. E. Pirhonen, and E. S. Husebye (1980), Crustal thicknesses in Fennoscandia, *Geophys. J. R. Astron. Soc.*, *63*, 759–774.
 Calcagnile, G. (1982), The lithosphere asthenosphere system in Fennoscandia, *Tectonophysics*, *90*, 19–35.
 Davis, J. L., J. X. Mitrovica, H.-G. Scherneck, and H. Fan (1999), Investigations of Fennoscandian glacial isostatic adjustment using modern sea level records, *J. Geophys. Res.*, *104*, 2733–2747.
 Dziewonski, A. M., and D. L. Anderson (1981), Preliminary Reference Earth Model (PREM), *Phys. Earth Planet. Inter.*, *25*, 297–356.
 Ekman, M. (1996), A consistent map of the postglacial uplift of Fennoscandia, *Terra Nova*, *8*, 158–165.
 Fjeldskaar, W., and L. Cathles (1991), The present rate of uplift of Fennoscandia implies a low-viscosity asthenosphere, *Terra Nova*, *3*, 393–400.
 James, T. S. (1991), Post-glacial deformation, Ph.D. thesis, Princeton Univ., Princeton, N. J.
 James, T. S., and A. Lambert (1993), A comparison of VLBI data with the ICE-3G glacial rebound model, *Geophys. Res. Lett.*, *20*, 871–874.
 Johansson, J. M., et al. (2002), Continuous GPS measurements of postglacial adjustment in Fennoscandia: 1. Geodetic results, *J. Geophys. Res.*, *107*(B8), 2157, doi:10.1029/2001JB000400.

Kaufmann, G., and K. Lambeck (2002), Glacial isostatic adjustment and the radial viscosity profile from inverse modeling, *J. Geophys. Res.*, *107*(B11), 2280, doi:10.1029/2001JB000941.
 Kaufmann, G., and P. Wu (2002), Glacial isostatic adjustment in Fennoscandia with a three-dimensional viscosity structure as an inverse problem, *Earth Planet. Sci. Lett.*, *197*, 1–10.
 Kaufmann, G., P. Wu, and G. Y. Li (2000), Glacial isostatic adjustment in Fennoscandia for a laterally heterogeneous Earth, *Geophys. J. Int.*, *143*, 262–273.
 Lambeck, K., C. Smither, and P. Johnston (1998), Sea-level change, glacial rebound and mantle viscosity for northern Europe, *Geophys. J. Int.*, *134*, 102–144.
 Latychev, K., J. X. Mitrovica, J. Tromp, M. E. Tamisiea, D. Komatitsch, and C. C. Christara (2005a), Glacial isostatic adjustment on 3-D Earth models: A finite volume formulation, *Geophys. J. Int.*, *161*, 421–444.
 Latychev, K., J. X. Mitrovica, M. E. Tamisiea, J. Tromp, and R. Moucha (2005b), Influence of lithospheric thickness variations on 3-D crustal velocities due to glacial isostatic adjustment, *Geophys. Res. Lett.*, *32*, L01304, doi:10.1029/2004GL021454.
 Martinec, Z. (2000), Spectral-finite element approach to three-dimensional viscoelastic relaxation in a spherical Earth, *Geophys. J. Int.*, *142*, 117–141.
 Martinec, Z., and D. Wolf (2005), Inverting the Fennoscandian relaxation-time spectrum in terms of an axisymmetric viscosity distribution with a lithospheric root, *J. Geodyn.*, *39*, 143–163.
 Milne, G. A., J. L. Davis, J. X. Mitrovica, H.-G. Scherneck, J. M. Johansson, M. Vermeer, and H. Koivula (2001), Space-geodetic constraints on glacial isostatic adjustment in Fennoscandia, *Science*, *291*, 2381–2385.
 Milne, G. A., J. X. Mitrovica, H.-G. Scherneck, J. L. Davis, J. M. Johansson, H. Koivula, and M. Vermeer (2004), Continuous GPS measurements of postglacial adjustment in Fennoscandia: 2. Modeling results, *J. Geophys. Res.*, *109*, B02412, doi:10.1029/2003JB002619.
 Mitrovica, J. X. (1996), *Haskell* [1935] revisited, *J. Geophys. Res.*, *101*, 555–569.
 Mitrovica, J. X., J. L. Davis, and I. I. Shapiro (1994), A spectral formalism for computing three-dimensional deformations due to surface loads: 2. Present-day glacial isostatic adjustment, *J. Geophys. Res.*, *99*, 7075–7101.
 Paulson, A., S. Zhong, and J. Wahr (2005), Modelling post-glacial rebound with lateral viscosity variations, *Geophys. J. Int.*, *163*, 357–371.
 Pérez-Gussinyé, M., A. R. Lowry, A. B. Watts, and I. Velicogna (2004), On the recovery of effective elastic thickness using spectral methods: Examples from synthetic data and from the Fennoscandian Shield, *J. Geophys. Res.*, *109*, B10409, doi:10.1029/2003JB002788.
 Poudjom Djomani, Y. H., J. D. Fairhead, and W. L. Griffin (1999), The flexural rigidity of Fennoscandia: Reflection of the tectonothermal age of the lithospheric mantle, *Earth Planet. Sci. Lett.*, *174*, 139–154.
 Ritsema, J., H. J. van Heijst, and J. H. Woodhouse (2004), Global transition zone tomography, *J. Geophys. Res.*, *109*, B02302, doi:10.1029/2003JB002610.
 Sandoval, S., E. Kissling, and J. Ansorge (2004), High-resolution body wave tomography beneath the SVEKALAPKO array—II. Anomalous upper mantle structure beneath the central Baltic Shield, *Geophys. J. Int.*, *157*, 200–214.
 Steffen, H., and G. Kaufmann (2005), Glacial isostatic adjustment of Scandinavia and northwestern Europe and the radial viscosity structure of the Earth’s mantle, *Geophys. J. Int.*, *163*, 801–812.
 Tushingham, A. M., and W. R. Peltier (1991), ICE-3G: A new global model of late Pleistocene deglaciation based upon geophysical predictions of postglacial relative sea level change, *J. Geophys. Res.*, *96*, 4497–4523.
 Watts, A. B. (2001), *Isostasy and Flexure of the Lithosphere*, Cambridge Univ. Press, New York.
 Wu, P., and W. van der Wal (2003), Postglacial sea levels on a spherical, self-gravitating viscoelastic Earth: Effects of lateral viscosity variations in the upper mantle on the inference of viscosity contrasts in the lower mantle, *Earth Planet. Sci. Lett.*, *211*, 57–68.
 Wu, P., H. Wang, and H. Schotman (2005), Postglacial induced surface motions, sea-levels and geoid rates on a spherical, self-gravitating laterally homogeneous Earth, *J. Geodyn.*, *39*, 127–142.
 Zhong, S., A. Paulson, and J. Wahr (2003), Three-dimensional finite element modeling of Earth’s viscoelastic deformation: Effects of lateral variations in lithospheric thickness, *Geophys. J. Int.*, *155*, 679–695.

R. Kendall, K. Latychev, and J. X. Mitrovica, Department of Physics, University of Toronto, 60 St. George Street, Toronto, ON, Canada M5S 1A7. (latychev@physics.utoronto.ca)

G. A. Milne and P. Whitehouse, Department of Earth Sciences, University of Durham, Science Labs, Durham DH1 3LE, UK. (pipa.whitehouse@durham.ac.uk)